THOR-AV 50th Percentile Male Biofidelity Evaluation in 25° and 45° Seatback Angle Test Conditions with a Semi-Rigid Seat

Z. Jerry Wang, Lauren W. Zaseck, Matthew P. Reed

Abstract THOR-AV, a modified THOR dummy, was developed to provide an immediate tool for the industry to evaluate the restraint system in automated driving system (ADS) equipped vehicles. The dummy was designed to address the non-traditional seated postures, submarining responses and rearward facing impact that the existing dummies were not designed for. The biofidelity evaluations were conducted and showed that the THOR-AV represented the human seated posture closely in both 25° and 45° seatback configurations. The responses of the restraint system had an overall BioRank scores (BRS) of 1.29 and 1.32 for 25° and 45° configurations, respectively, both corresponding to *good* biofidelity. The responses of THOR-AV had *excellent* biofidelity in both test configurations with overall BRS scores of 0.73 and 0.89 for 25° and 45° configurations, respectively. The dummy was durable, and no damage was observed from the test series. The dummy was released as standard build level A (SBL-A) by Humanetics and is ready for use to evaluate the restraint system in ADS-equipped vehicles in forward facing seating configurations.

Keywords Automated Driving System, Biofidelity, Reclined Seat, Semi-rigid seat, THOR-AV.

I. INTRODUCTION

Automated Driving System technology has made significant advancement in the past decade with breakthroughs in machine learning and neural network technologies. ADS-equipped vehicles have been tested for years and the technology is maturing and is expected to become part of our daily transportation in the foreseeable future. With an ADS-equipped vehicle, occupants may be able to choose different seating configurations [1-2], for example, reclined seat for resting, rearward facing to face others for social interaction, etc. However, only the traditional forward-facing position with a seatback angle at approximately 25° is currently required for safety testing. It is unknown if the restraint system would provide similar protection to the occupants when seated in reclined, oblique impact, rearward facing, or a combination of any of these scenarios. In 2019, National Highway Traffic Safety Administration (NHTSA) initiated a research program to study ADS-equipped vehicle occupant kinematics (AVOK), aiming to provide fundamental biomechanical guidance to develop suitable anthropomorphic test devices (ATDs) and related injury criteria for restraint system evaluation. The program consists of forward-facing Post-Mortem Human Subject (PMHS) tests in upright and reclined seated postures for midsize male PMHS and more-vulnerable occupants such as small females and obese occupants. Rearward facing PMHS tests with frontal crash severity were conducted in upright and reclined seated postures by the Ohio State University (Columbus, Ohio) and the THOR-AV was evaluated in this these test conditions recently [3]. The research contract for the forward-facing male was awarded to the University of Michigan Transportation Research Institute (UMTRI, Ann Arbor, Michigan, USA). The tests used a sled with a semi-rigid buck developed by [4] with the seatback at 25° and 45° configurations. Three PMHS tests were conducted for each configuration.

THOR-AV 50M (THOR-AV hereafter) is a modified THOR-50M ATD developed by Humanetics Innovative Solutions (Humanetics, Farmington Hills, Michigan, USA) to meet the immediate need for restraint system evaluation in ADS-equipped vehicles (AV). The THOR-AV design was intended to improve the seated postures in a reclined seat, neck torsion and extension biofidelity, and submarining responses. THOR-AV has a new neck design that was developed by [5] with improved biofidelity over THOR and Hybrid III 50th dummies, especially the torsion responses. It has an updated pelvis bone and flesh geometry based on the most recent study defined in

Dr. Z. J. Wang is the Chief Technology Officer of Humanetics Innovative Solutions, Inc., USA, (tel: +1 248 778 2133, email: jwang@humaneticsatd.com). Dr. L. W. Zaseck is an Assistant Research Scientist and Dr. M. P. Reed is a Research Professor and Head of the Biosciences Group at The University of Michigan Transportation Research Institute (UMTRI), USA.

[6]. The two abdomen InfraRed – Telescoping Rod for Assessment of Chest Compression (IR-TRACCs) were replaced by Abdomen Pressure Twin Sensors (APTS). There are improvements in the coupling between pelvis flesh and pelvis bone, and between thigh and pelvis fleshes [7]. The dummy also has a refined Anterior Posterior Iliac Spine (ASIS) profile [8] and a cavity underneath the pelvic bone to provide proper pelvis compression and match the human hip joint height.

The study in this paper focused on evaluation of the THOR-AV in forward facing, upright right and reclined test conditions. The objective is to evaluate THOR-AV biomechanical responses in UMTRI AVOK sled test conditions at a seatback angle of 25° and 45°.

II. METHODS

The tests were conducted at the University of Michigan Transportation Research Institute with the same sled buck that was used for the PMHS tests [3]. The seat was a semi-rigid seat used in [9] with additions of two dampers to the anti-submarining ramp. A 10-camera system was used to capture the motions of the dummy. The trajectories of the interest points were analyzed with TEMA software (Image Systems AB, Sweden).

Test Setup

The test setup consisted of supporting frames and a semi-rigid seat. The back of the dummy was supported with seat belt webbing, which provided the maximum view clearance for the cameras. The semi-rigid seat is shown in Fig. 1. The seat consists of a rigid base plate pivoted at the rear edge. It had two front springs to provide stiffness similar to the front production seat. There was an anti-submarining plate at the front, which was pivoted at the front edge of the seat pan. The anti-submarining plate was coupled with a spring damping system that can provide stiffness like a production seat [9].

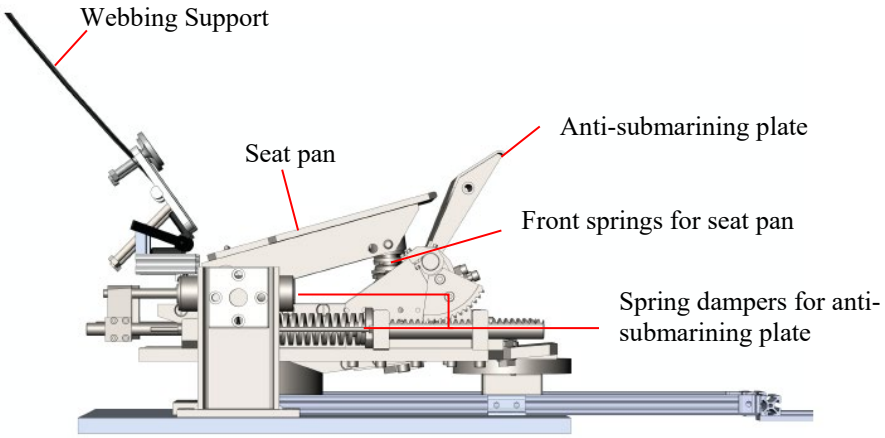

Fig. 1. Semi-rigid seat [4] as constructed by UMTRI.

The test buck is shown in Fig. 2. The buck had a rigid toe pan. A knee bolster plate was installed with a foam pad cover at the front. The knee bolster was far away from the dummy in setup and was purposely built to prevent the dummy from damage in case it was not properly restrained during the test. In a normal test, the knee would not contact the knee bolster.

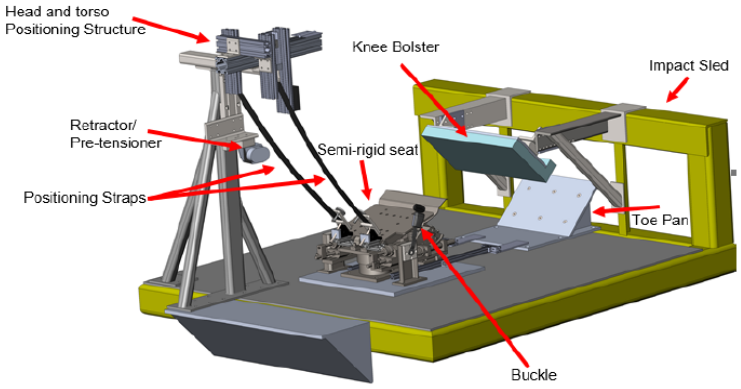

Fig. 2. Test buck layout.

The belt system was provided by ZF North America, Inc. The belt system was equipped with a dynamic-locking latch plate and a combined retractor pretensioner/load limiter, with a load limit of approximately 3.5 kN. The shoulder belt location was adjusted to simulate a seat-mounted retractor, so the position of the retractor relative to the shoulder was similar across recline angles. The shoulder belt was placed to cross the middle of the clavicle. The lap belt was routed low on hips, touching the thighs. The belt was snug and as close to the bones as possible.

Instrumentation

A THOR-50M dummy was converted to THOR-AV with a conversion kit. The sensors installed on the dummy are listed in TABLE I.

TABLE I
THOR-AV SENSOR LIST

Location	Sensors	Make/Model
Head	Linear accelerometers (x,y,z)	Endevco 7264C-2000
	Angular rate sensor (x,y,z)	DTS ARS-PRO-18K
Neck pot	Rotary potentiometer	HIS 9945
Neck	Upper neck load cell	HIS IH-11980J
Clavicle	Clavicle load cell left	HIS IH-10925J
	Clavicle load cell right	HIS IH-10935J
Spine	Upper thoracic spine load cell	HIS IH-12010J
	Thoracic spine load cell	HIS 10415JI4
T1, T4, T12	Linear accelerometers (x,y,z)	Endevco 7264C-2000
T4	Angular rate sensors (x,y,z)	DTS ARS-PRO-18K
Sternum	Linear accelerometer (x)	Endevco 7264C-2000
Thorax	IR-TRACCS (UL, UR, LL, LR)	HIS IF-364-C-R5
	Potentiometers (2 per IR-TRACC)	HIS 9945
Abdomen	Pressure sensors (2)	Transpolis 50 mm dia x 141.50 mm
Pelvis	Linear accelerometers (x,y,z)	Endevco 7264C-2000
	Angular rate sensors (x,y,z)	DTS ARS-PRO-18K
	ASIS load cell left	HIS IH-12020J
	ASIS load cell right	HIS IH-12030J
	Acetabulum load cell, left	HIS IH-11990J
	Acetabulum load cell, right	HIS IH-12000J
Thigh	Femur load cell left & right	HIS W50-71010
Leg	Upper tibia load cell left & right	HIS 10390JI4
	Lower tibia load cell right	HIS 10391JI4
	Achilles load cell left and right	HIS 10389J

The sled at UMTRI is a 450-kilogram, 2 meter-square platform that travels on an 18-meter track. The sled is accelerated by a pneumatically powered ram from one end of the track, while the impact event takes place at the opposite end. A pneumatic cylinder controls the duration and magnitude of the impact event. The instrumentation installed on the sled are listed in TABLE II. Both belt anchors at the belt buckle side and anchor side were instrumented with 3-axis load cells.

TABLE II
SLED INSTRUMENTATION

Location	Sensor	Make/Model
Seat Front	Load Cell	HIS DN 2881TF
Seat Rear	Load Cell	HIS DN 2513
Belt Anchors	Load Cell	HIS DN 2881TF
Sled	Accelerometer	PCB, 3741F12200G
	Accelerometer	Endevco A7232
Seat IC	Accelerometer	Endevco 7264C-2000
Cameras System (2000 fps)	Camera 1-6	NAC Memrecam GX-1
	Camera 7-8	Redlake HG100k
	Camera 9	Redlake HG-LE
	Camera 10	IDT N3

Sled Pulse

The sled test had a delta velocity of 32 km/h. The sled pulse is shown in Fig. 3 below.

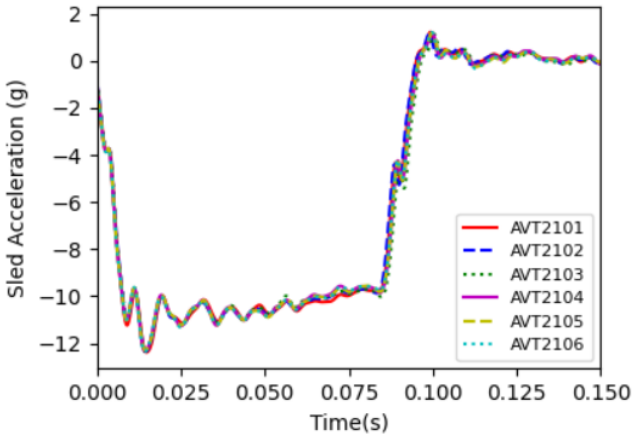

Fig. 3. Sled acceleration for the biofidelity evaluation test.

Test Matrix

There was a total of six THOR-AV tests conducted in this study, three repeats for each configuration. The test matrix is summarized in TABLE III.

TABLE III
THOR-AV TEST MATRIX

Seatback Angle	Test 1	Test 2	Test 3
25°	AVT2101	AVT2102	AVT2103
45°	AVT2104	AVT2105	AVT2106

Data Processing Method

The sensor data were sampled with a 20,000Hz sampling rate. The video data was sampled at 2,000 frame per second. All data channels were filtered as specified in SAE J211 except for the head and pelvis accelerations. Instead of CFC1000 as specified in SAE J211, CFC180 was used to be consistent with the filter used for PMHS data. Trajectory data was processed with TEMA software from the video data. No filters were applied to the trajectory data.

PMHS Data Corridors

The PMHS test data were downloaded from NTHSA Biomechanics Database [4]. There were 3 PMHS tests for each test configuration. The standard deviation and the average were calculated for the time history data. The upper boundary of each PMHS corridor was derived with the average of the three tests plus their one standard deviation. The lower boundary of each PMHS corridor was calculated with the average of the three tests minus their one standard deviation.

BioRank Calculation

The BioRank scores (BRS) calculation method has been developed by NHTSA [10-13] and improved and refined through the years in each publication. The latest method was documented in [14-15]. To calculate the BioRank scores for THOR-AV, the same process used in THOR calculations for the corresponding data channels was followed, including PMHS corridor duration and the data curve alignment method. The Dummy Phase Shift (DPS) was not included in the BRS calculation but being monitored.

The dummy BRS scores were grouped by body segment, which are outlined in Fig. 4 and Fig. 5, respectively.

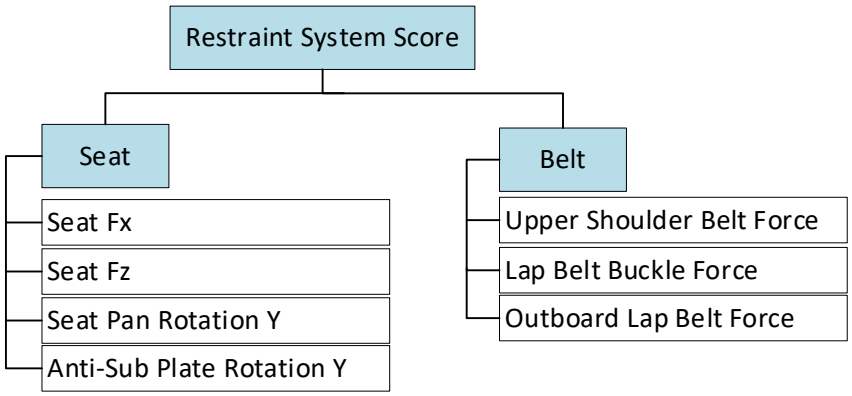

Fig. 4. Components for restraint system BRS scores.

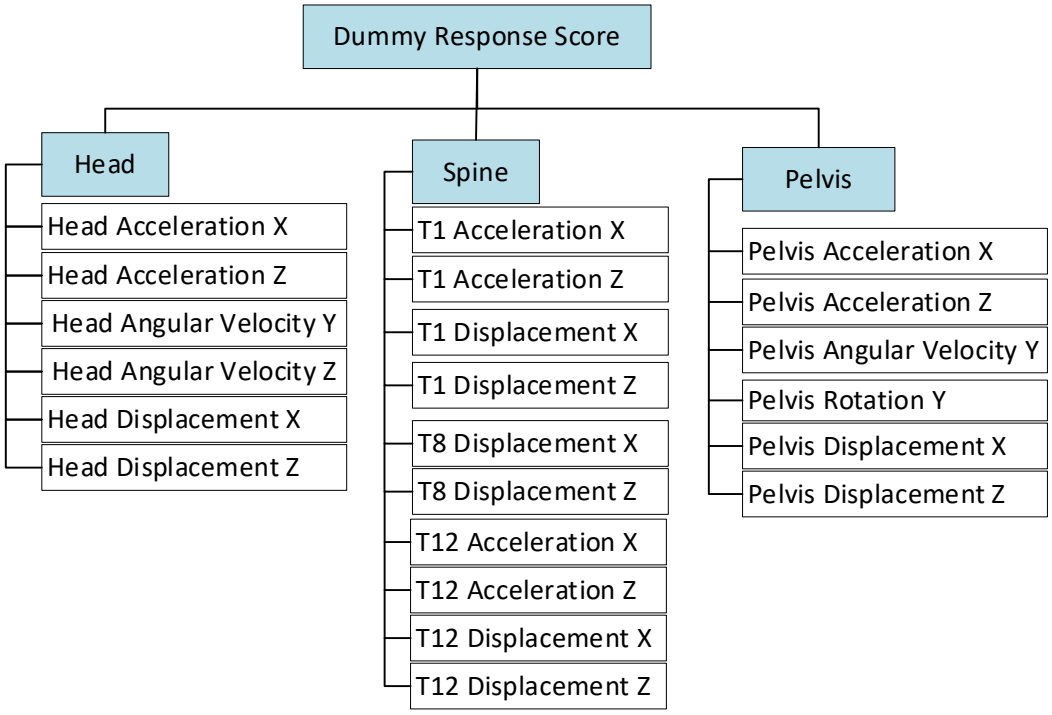

Fig. 5. Components for THOR-AV BRS scores.

If the BRS was less or equal than 1.0, the biofidelity was considered *excellent*. If the BRS was greater than 1.0, but less or equal to 2.0, the biofidelity was considered *good*. If the BRS was greater than 2.0, but less or equal to 3.0, the biofidelity was considered *marginal*. If the BRS was greater than 3.0, the biofidelity was considered *poor*. The relationship between biofidelity and BRS scores are summarized in TABLE IV.

TABLE IV
BIORANK SCORE RANGE AND BIOFIDELITY CORRELATION

BRS Scores	BRS ≤ 1.0	1.0 <BRS ≤ 2.0	2.0 <BRS ≤ 3.0	BRS > 3.0
Biofidelity	*Excellent*	*Good*	*Marginal*	*Poor*

III. RESULTS

The THOR-AV dummy was evaluated in the following categories: dummy positioning, submarining responses and biofidelity ranking. The plots in the Appendix consist of data that were available from both PMHS tests and the THOR-AV tests.

Dummy Positioning

One outcome of interest is how closely the dummy could be positioned to the human-derived targets. The dummy positioning was evaluated against the PMHS specimen results, which followed the volunteer prediction model in [16]. Since the body segment angles measured in the PMHS tests referenced the anatomical landmarks which were not easy to identify in a dummy, the THOR-AV was configured to match the seated postures corresponding to the PMHS in the 3-D CAD model, and the target tilt sensor angles were mapped out and used as a guidance for dummy positioning. The PMHS body segment angles and their corresponding tilt sensor angles are summarized in TABLE V for 25° seatback, and TABLE VI for 45° seatback.

TABLE V
TILT SENSOR ANGLES FOR THOR-AV SETUP AT 25° SEATBACK

	PMHS	Corresponding Tilt Angles for THOR-AV	AVT2101	AVT2102	AVT2103	Average
Pelvis	54.6°	33.2°	35.7°	36.2°	36.1°	36.0°
T8		21.2°	29.1°	29.5°	29.2°	29.3°
T1	13.3°	4.2°	6.9°	5.9°	6.9°	6.6°
Head	7.3°	0.6°	-2.4°	-2.3°	-2.4°	-2.4°

TABLE VI
TILT SENSOR ANGLES FOR THOR-AV AT 45° SEATBACK

	PMHS	Corresponding Tilt Angle for THOR-AV	AVT2104	AVT2105	AVT2106	Average
Pelvis	65.0°	39.9°	41.6°	42.8°	41.6°	42.0°
T8		45.9°	49.1°	49.4°	48.6°	49.0°
T1	33.5°	28.9°	27.5°	28.9°	26.5°	27.6°
Head	23.8°	25.3°	24.2°	23.1°	23.0°	23.4°

Submarining

In both the 25° and 45° configurations, no submarining was observed for the THOR-AV, which was consistent with the PMHS response. The videos were reviewed carefully and confirmed no submarining occurred. In addition, the lap belt data and the ASIS loads were reviewed, and no sudden force drop was present either.

Biofidelity

The biofidelity was assessed with the NHTSA BioRank calculation method outlined in [14]. The BRS scores are summarized in TABLE VII for the restraint system in the 25° and 45° seatback configurations. The BRS scores for the seat were 1.53 and 1.64 for the 25° and 45° seatback, respectively, both corresponding to *good* biofidelity. The BRS scores for the belt system were 1.05 and 0.99 for the 25° and 45° seatback respectively, corresponding to *good* and *excellent* biofidelity. The anti-submarining bar rotation both had *marginal* and *poor* biofidelity with BRS scores of 2.99 and 3.46 for the 25° and 45° seatback, respectively.

TABLE VII
RESTRAINT SYSTEM BRS SCORES FOR THE 25° AND 45° SEATBACK CONFIGURATIONS

Seatback Angle	25°		45°	
Restraint System	BRS	DPS (ms)	BRS	DPS (ms)
Seat	1.53	-3	1.64	0
Seat Fx	1.19	-2	1.75	0
Seat Fz	1.30	-5	0.72	-1
Seat Pan Rotation Y	0.62	-4	0.63	0
Anti-submarining Bar Rotation Y	2.99	0	3.46	0
Belt	1.05	-6	0.99	-5
Outer Lap Belt Force	0.79	-9	1.22	-10
Lap Belt Buckle Force	1.42	-8	0.93	-6
Shoulder Belt Force	0.94	0	0.82	2
Average	1.29	-4	1.32	-3

The THOR-AV dummy response BRS scores for the 25° and 45° seatback configurations are summarized in TABLE VIII. The head BRS scores were 0.54 and 0.83 for the 25° and 45° seatback configurations, respectively, both corresponding to *excellent* biofidelity. The spine has BRS scores of 0.78 and 0.62 for the 25° and 45° seatback configurations, respectively, both corresponding to *excellent* biofidelity. The pelvis BRS scores were 0.87 and 1.23 for the 25° and 45° seatback configurations, respectively, corresponding to *excellent* and *good* biofidelity. The overall THOR-AV BRS scores are 0.73 and 0.89 for the 25° and 45° seatback configurations, respectively, both corresponding to *excellent* biofidelity.

TABLE VIII
THOR-AV BRS SCORES FOR THE 25 AND 45 SEATBACK CONFIGURATIONS

Seatback Angle	25°		45°	
THOR-AV	BRS	DPS (ms)	BRS	DPS (ms)
Head	0.54	1	0.83	0
Head Acceleration X	0.66	-3	0.88	0
Head Acceleration Z	0.76	-1	1.12	0
Head Angular Velocity Y	0.82	6	1.45	4
Head Displacement X	0.20	-2	0.11	-4
Head Displacement Z	0.28	4	0.60	-1
Spine	0.78	0	0.62	-1
T1 Acceleration X	0.77	-1	0.61	0
T1 Acceleration Z	1.35	0	0.75	0
T1 Displacement X	0.34	0	0.67	-3
T1 Displacement Z	1.42	0	0.28	6
T8 Displacement X	0.28	0	0.77	-3
T8 Displacement Z	0.65	0	0.57	0
T12 Acceleration X	0.84	0	0.80	-3
T12 Acceleration Z	0.76	0	0.80	0
T12 Displacement X	1.00	0	0.32	-3
T12 Displacement Z	0.38	0	0.58	0
Pelvis	0.87	0	1.23	-1
Pelvis Acceleration X	1.21	0	1.56	0
Pelvis Acceleration Z	0.70	0	0.85	-1
Pelvis Angular Velocity Y	0.74	0	1.15	-3
Pelvis Rotation Y	0.77	0	1.35	0
Pelvis Displacement X	0.64	0	NA	NA
Pelvis Displacement Z	1.14	0	NA	NA
Average	0.73	0	0.89	-1

IV. DISCUSSION

For the restraint system, THOR-AV had BRS scores 1.29 and 1.32 for the 25° and 45° seatback configurations, respectively, both corresponding to *good* biofidelity. The seat forces for the THOR-AV matched the responses of the PMHS closely, but on the high side of the PMHS corridors, shown in Fig. A1 and Fig. A2 in the Appendix. This was most likely due to the lighter PMHS body mass than the THOR-AV. Similar relationships were observed for the seat pan rotation. The anti-submarining plate rotation for THOR-AV had *marginal* or *poor* biofidelity in both test configurations. The magnitude of the rotations was nearly twice as high as the PMHS responses, shown in Fig. A4. The PMHS specimens were elderly and had thinner thigh flesh than the THOR-AV dummy, which was designed to represent a 50th percentile 45-year-old male. The ATD flesh is also stiffer and more tightly coupled than human flesh, which may affect the pattern of loading on the seat. The inboard lap belt force was measured at the buckle anchor joint, and the outer belt force was measured at the anchor joint. The belt had an overall BRS score of 1.05 and 0.99 for the 25° and 45° seatback, respectively, corresponding to *good* and *excellent* biofidelity. The lap belt and the shoulder belt force matched the PMHS corridors reasonably well, shown in Fig. A5 through Fig. A7.

The THOR-AV dummy performed well against the PMHS responses with BRS scores 0.73 and 0.89 for the 25° and 45° configurations, respectively, both corresponding to *excellent* biofidelity. The head biofidelity was *excellent* with BRS scores of 0.54 and 0.83 for the 25° and 45° configurations, respectively. The head z-acceleration reached the peak value by 25 ms later than the PMHS and the magnitudes of peaks were close, shown in Fig. A9. The delay implied a less-coupled upper and lower torso (the THOR-AV has a more flexible lumbar and thoracic spine than THOR). Head y-angular velocity had a lower peak magnitude than PMHS response in both the 25° and 45° configurations, shown in Fig. A11. The head z-angular velocity matched the PMHS very well (shown in Fig. A12) in both test configurations, which benefitted from the torsion element design in the THOR-AV neck.

T1 and T12 x-accelerations matched the PMHS responses very well in both test configurations, shown in Fig. A14and Fig. A17, respectively, as are the resultant accelerations at the T1 and T12, shown in Fig. A16 and Fig. A19.

The pelvis x-acceleration matched the PMHS response closely for the 25° configuration (shown in Fig. A20, left). The first peak value for the 45° configuration had a 25-ms delay compared to the PMHS response, though its peak magnitude matched the PMHS (shown in shown in Fig. A20, right). Again, this implied a less coupled upper and lower torso. The pelvis z-accelerations matched the PMHS responses very closely in both test configurations, shown in Fig. A21. For pelvis y-angular velocity, the THOR-AV pelvis matched the PMHS response in the 25° configuration though it was on the low side of the PMHS corridor. The THOR-AV y-angular velocity in the 45° configuration was lower than the PMHS responses (shown in Fig. A23). The rotation of the pelvis was calculated by integrating the pelvis angular velocity in the y-direction. The pelvis y-rotation was within the PMHS corridors for the 25° configuration (Fig. A24, left), and slightly outside the PMHS corridor for the 45° configuration Fig. A24, right).

Displacement in x- and z-direction were evaluated for the head, T1, T8, T12 and the pelvis. The THOR-AV head x- and z-displacement were well within the PMHS corridors for both test configurations, and all showed *excellent* biofidelity, shown in Fig. A25 and Fig. A26. The T1 x-displacement matched the PMHS response very well for both test configurations (Fig. A27), showing *excellent* biofidelity. The T1 z-displacement was slightly higher than the PMHS corridors for the 25° test configuration Fig. A28, left), but well within the PMHS corridor for the 45° test configuration (Fig. A28, right). The T8 and T12 displacements in x- and z-direction matched the PMHS reasonably well (shown in Fig. A29 and Fig. A30), in both test configurations. For the pelvis x-displacement in both test configurations, the THOR-AV responses matched the PMHS responses fairly well (Fig. A23). Unfortunately, the target block on the pelvis was sheared off in the first test of the 45° configuration, and there was not enough time to work out an alternative solution during the testing. Only a portion of the pelvis x-displacement data was available (up to 60 ms approximately, Fig. A33, right) and it stayed well within the PMHS corridor. The pelvis z-displacement was low for both test configurations because the lap belt restrained the pelvis from moving (Fig. A34).

The work presented in this paper was part of a series of studies regarding the biofidelity of THOR-AV. The neck biofidelity in forward, lateral, torsion and oblique test condition was published last year[5]. Evaluations for rear-facing was published early this year [3]. The upright front and rear seat configurations are being published simultaneously [7]. The authors are not aware of any research for full body PMHS test in oblique test condition but hope it would happen in the future as it is an important biofidelity criteria.

V. CONCLUSIONS

The THOR-AV 50M dummy was developed for restraint system evaluation in upright, reclined seat, forward facing, rearward facing and oblique impact conditions. This study evaluated the biofidelity of THOR-AV in the 25° seatback (upright) and 45° seatback (reclined) configurations in a forward-facing crash scenario as part of a series of studies regarding the THOR-AV biofidelity. The dummy was evaluated against the PMHS and volunteer seated posturers. It matched human seated postures well. The evaluation showed that THOR-AV had *good* biofidelity for restraint system response with the overall BRS scores of 1.29 and 1.32 for the 25° and 45° test configurations, respectively. The THOR-AV responses showed *excellent* biofidelity with the overall BRS scores of 0.73 and 0.89 for the 25° and 45° test configurations, respectively. The dummy showed good durability and no damage was observed in this test series. The THOR-AV dummy was released as standard build level A (SBL-A) and is available for use by industry for restraint system assessment. As new PMHS data is available in the future, the THOR-AV dummy will be further evaluated and enhanced where necessary.

VI. ACKNOWLEDGEMENT

The authors would like to express their gratitude to the staff in the UMTRI sled lab, Mr. Carl Miller, Ms. Anne Bonifas, Mrs. Nicole Orton, and Mr. Kyle Boyle, who conducted the tests. We are also very grateful to Humanetics engineering team, especially Mr. Brian Loeber and Ms. Emily Bastian who provided technical assistance and coordination for the dummy preparation and certification before testing.

VII. REFERENCES

[1] Jorlöv J. Bohman K., Larsson A. Seating positions and activities in highly automated cars – a qualitative study of future automated driving scenarios, *IRCOBI Conference Proceedings*, September 13-15, 2017, Antwerp, Belgium.

[2] Lopez-Valdes F., Jimenez-Octavio J., Bohman K., Logan D., Raphael W., Jimenez L., Koppel S., Seating preferences in highly automated vehicles are dependent on yearly exposure to traffic and previous crash experiences, *IRCOBI Conference Proceedings*, Florence, Italy, September 11-13, 2019.

[3] Wang, Z.J., Biomechanical Responses of the THOR-AV ATD in rear facing test conditions, *SAE World Congress, 2022,* SAE Technical Paper 2022-01-0836, 2022. https://doi.org/10.4271/2022-01-0836

[4] NHTSA Test Report, https://www.nhtsa.gov/research-data/research-testing-databases#/biomechanics. Test numbers 12795, 12796, 13109, 13110, 13119, 13124.

[5] Wang, Z.J., Loeber B., Tesny A., Hu G., Kang Y.S., Neck biofidelity comparison of THOR-AV, THOR and Hybrid III 50th dummies, *IRCOBI Conference Proceedings*, September 8-10, 2021, online.

[6] Reed M.P., *Development of anthropometric specifications for warrior injury assessment manikin*, report number UMTRI-2013-38, October 2013.

[7] Wang, Z.J., Richard O., Lebarbé M., Kabadayi E., Kleessen C., Biomechanical responses of THOR-AV in semi-rigid seat that mimics the front and rear seat, *IRCOBI Conference Proceedings*, September 14-16, 2022, Porto, Spain

[8] Muehlbauer J, Pfeiffer N, Puschnig M, Schick S, Bayerschen E, Peldschus S, 2020. Distribution of Anterior Iliac Wings Geometries in the Population and Comparison to Finite Element Human Body Models, 2020 *IRCOBI Conference Proceedings*, Munich, Germany (virtual).

[9] Uriot J., Potier P., Baudrit P., Trosseille X., Petit P., Richard O., Compigne S., Masuda M., Douard R., 2015. Reference PMHS sled tests to assess submarining. *Stapp Car Crash Journal*, Vol. 59, pp 203-224.

[10] Rhule H.R., Maltese M.P., Donnelly B.R., Eppinger R.H., Brunner J.K. and Bolte IV J.H., Development of a new biofidelity ranking system for anthropomorphic test devices, *Stapp Car Crash Journal*, 46th Stapp Car Crash Conference (November 2002), pp. 477-512.

[11] Rhule H., Moorhouse K., Donnelly B., Stricklin J., Comparison of WorldSID and ES-2RE biofidelity using an updated biofidelity ranking system, *21st International Technical Conference on Enhanced Safety of Vehicles* (ESV), Stuttgart, Germany, June 2009.

[12] Rhule H., Donnelly B., Moorhouse K., Kang Y-S., A methodology for generating objective target for quantitively assessing the biofidelity of crash test dummies, *23rd International Technical Conference on Enhanced Safety of Vehicles (ESV)*, Seoul, Korea, May 27-30, 2013.

[13] Rhule H., Stricklin J., Moorhouse K., Donnelly B., Improvements to NHTSA's biofidelity ranking system and application to the evaluation of the THOR 5th female dummy, *IRCOBI Conference Proceedings*, 2018, paper # IRC-18-12.

[14]Kang Y-S., Stammen J., Ramachandra R., Agnew R.M. Hagedorn, A., Thomas C., Kwon H.J., Moorhouse K., Bolte IV J.H., Biomechanical responses and injury assessment of post-mortem human subjects in various rear-facing seating configurations. *Stapp Car Crash Journal*, vol. 64 (November 2020), pp. 155-212.

[15]Hagedorn A., et al. Biofidelity evaluation of THOR-50M in rear-facing seating configurations using an updated BioRank system, *SAE International Journal of Transportation Safety* (February 2022), Special Issue: Occupant Protection & Crashworthiness for ADS-Equipped Vehicles.

[16]Reed M.P., Ebert S.M., Jones M.L.H., Posture and belt fit in reclined passenger seats, *Traffic Injury Prevention*, 2019, vol. 20, No. S1, S28-S42.

VIII. APPENDIX

The plots of the THOR-AV test results and the PMHS corridors are presented in this Appendix.

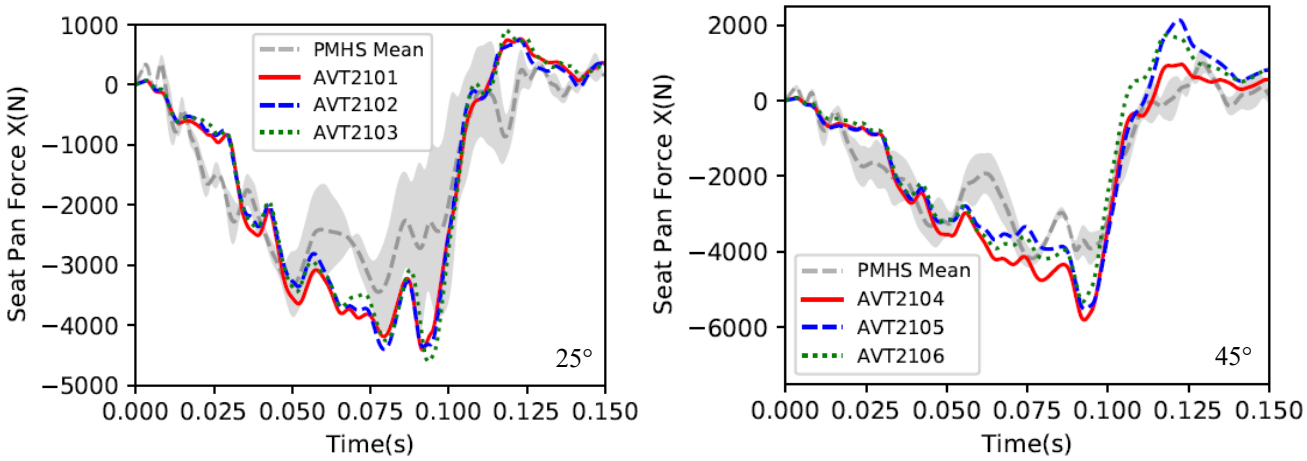

Fig. A1. Seat pan force x for the 25° (left) and 45° (right) configurations.

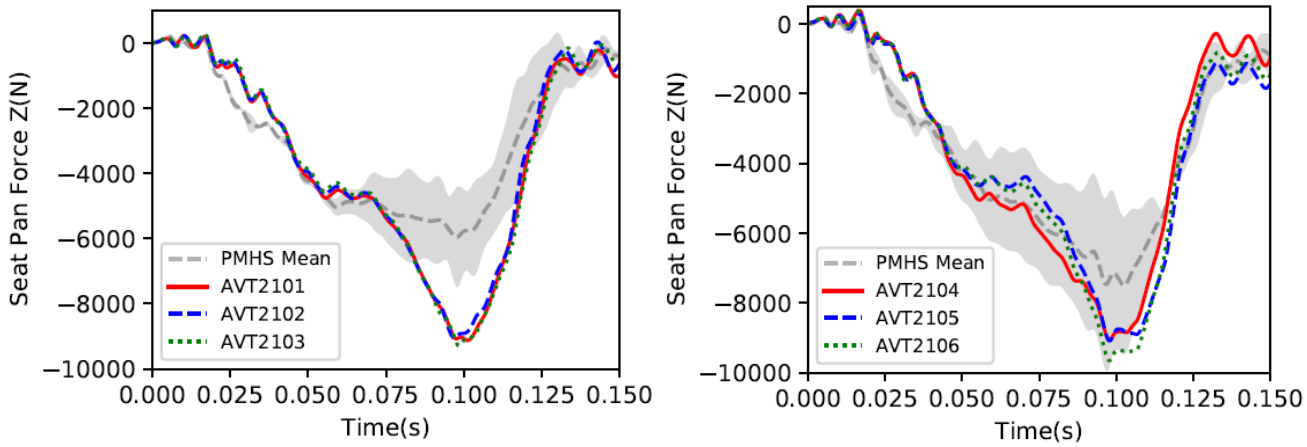

Fig. A2. Seat pan force Z for the 25° (left) and 45° (right) configurations.

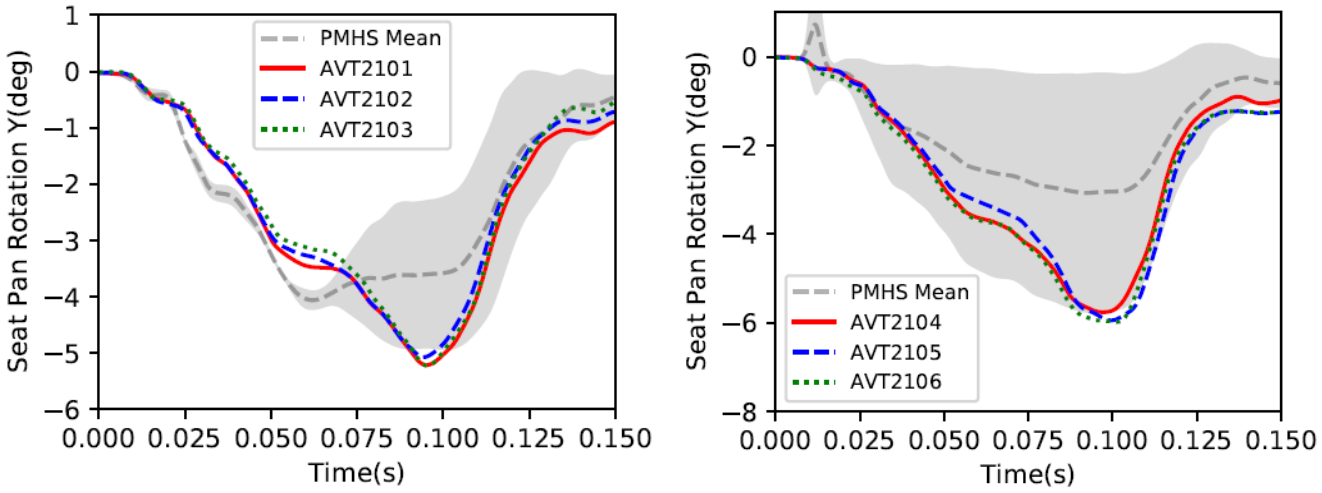

Fig. A3. Seat pan rotation Y for the 25° (left) and 45° (right) configurations.

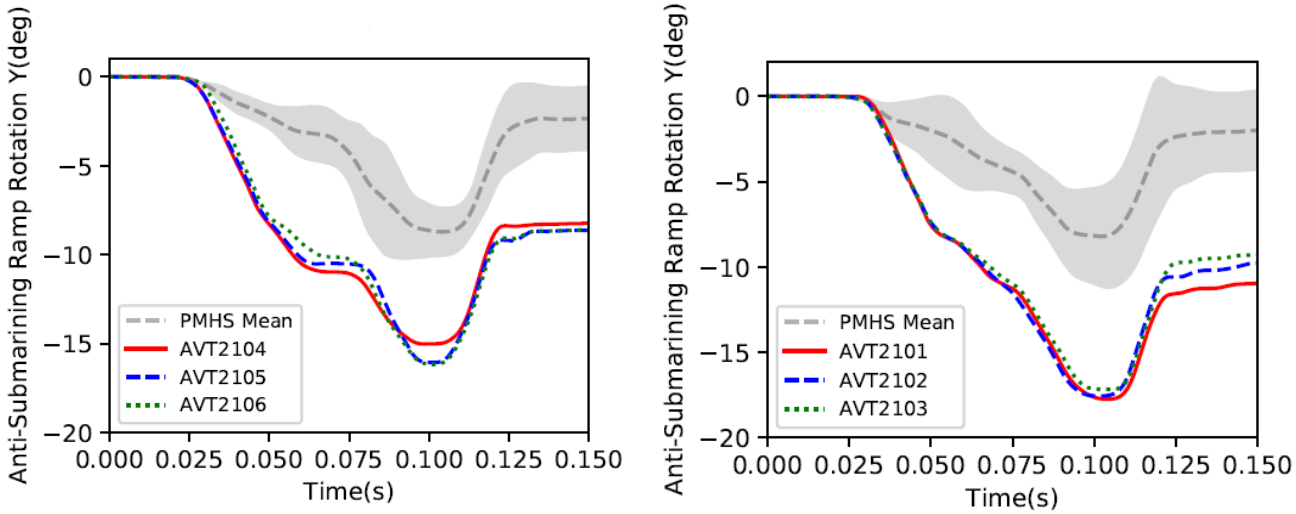

Fig. A4. Anti-submarining Ramp Rotation Y for the 25° (left) and 45° (right) configurations.

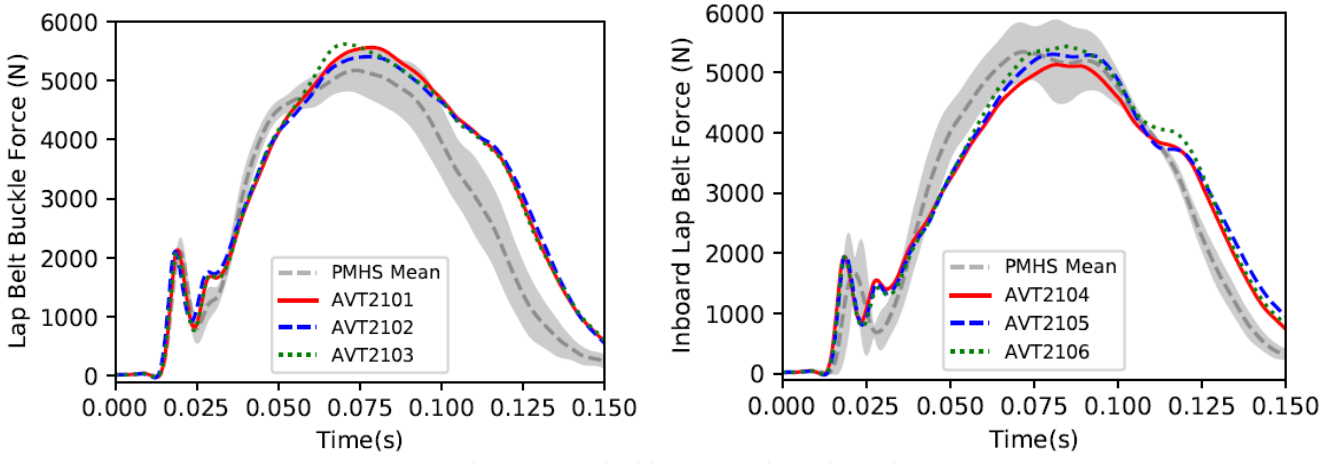

Fig. A5. Lap belt Force at buckle anchor for the 25° (left) and 45° (right) configurations.

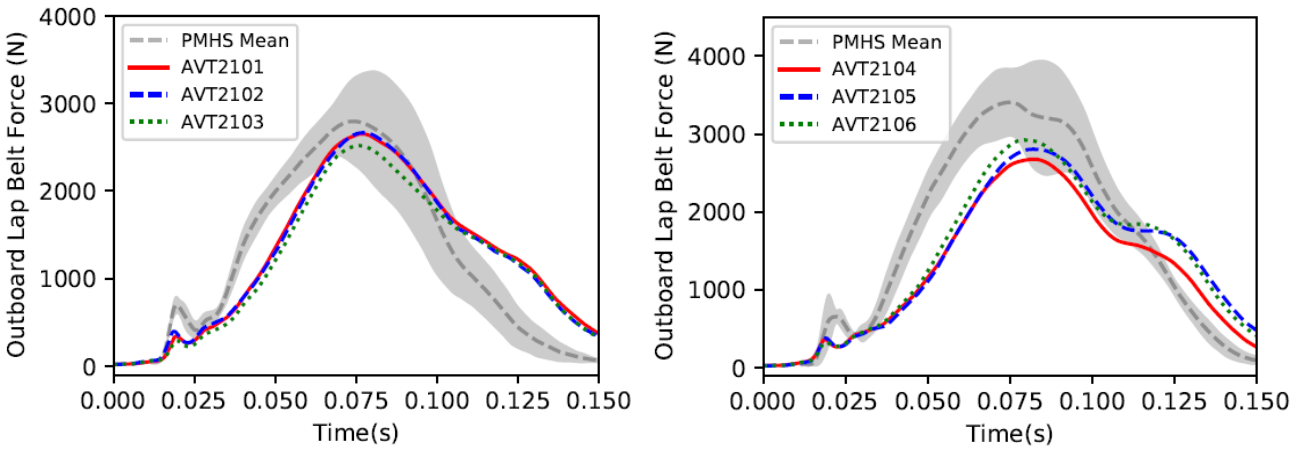

Fig. A6. Outboard lap belt force for the 25° (left) and 45° (right) configurations.

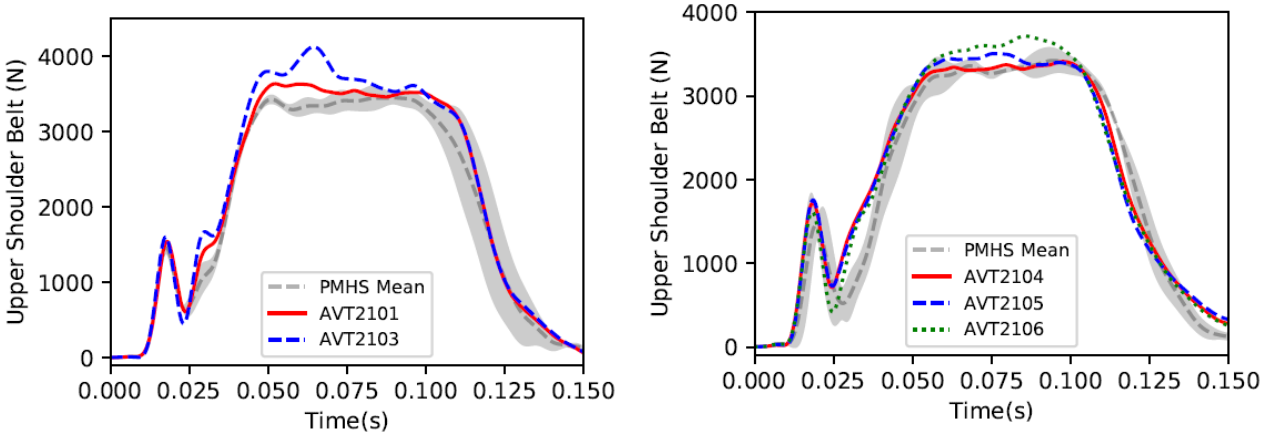

Fig. A7. Upper shoulder belt force for the 25° (left) and 45° (right) configurations.

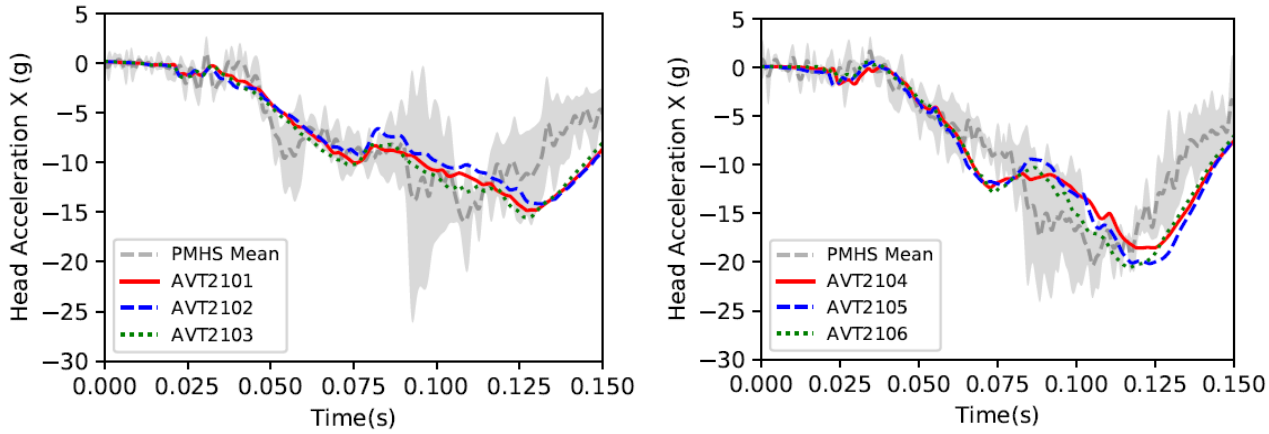

Fig. A8. Head acceleration X for the 25° (left) and 45° (right) configurations.

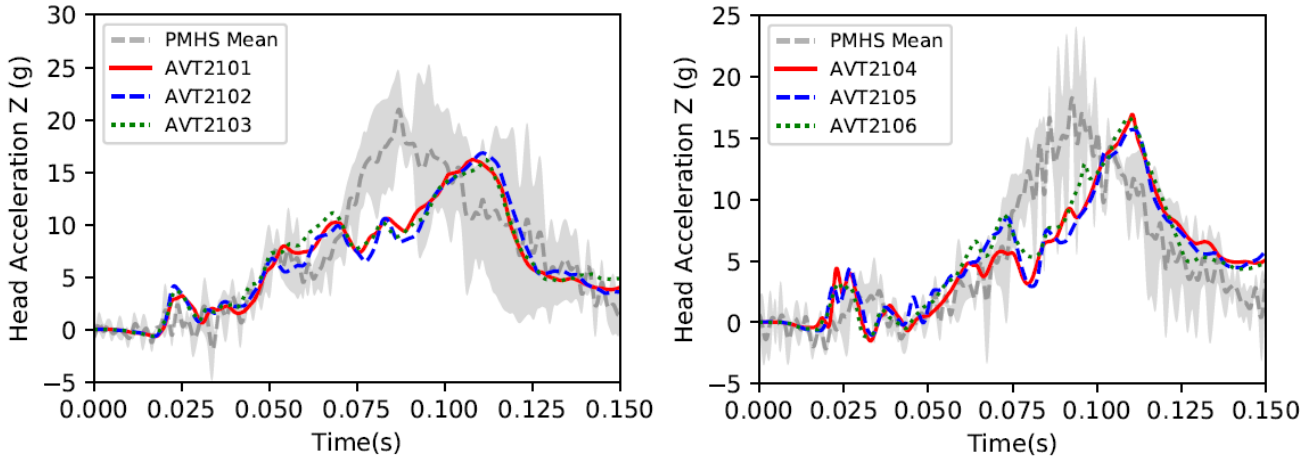

Fig. A9. Head acceleration Z for the 25° (left) and 45° (right) configurations.

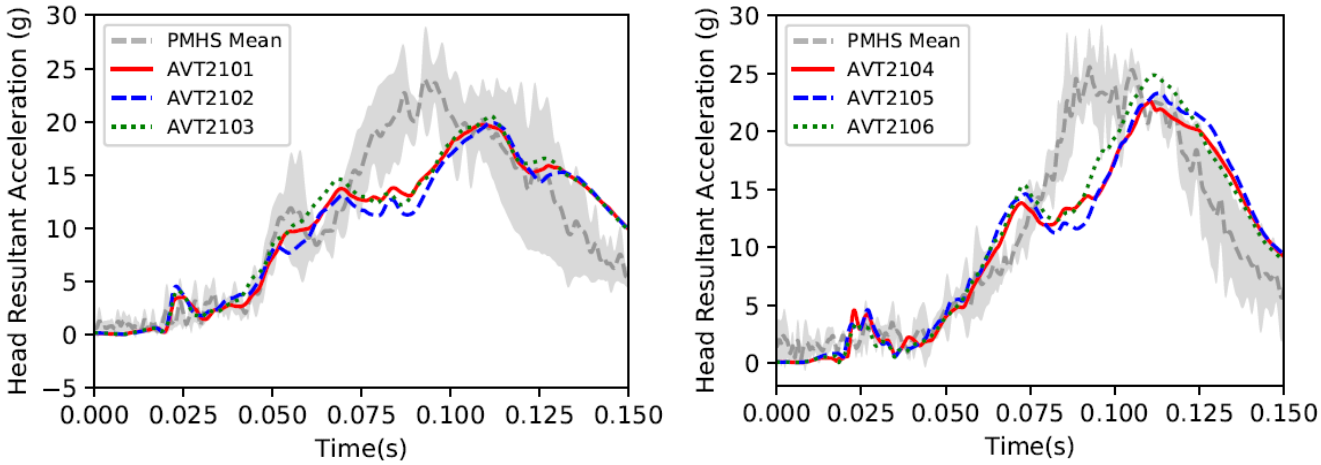

Fig. A10. Head resultant acceleration for the 25° (left) and 45° (right) configurations.

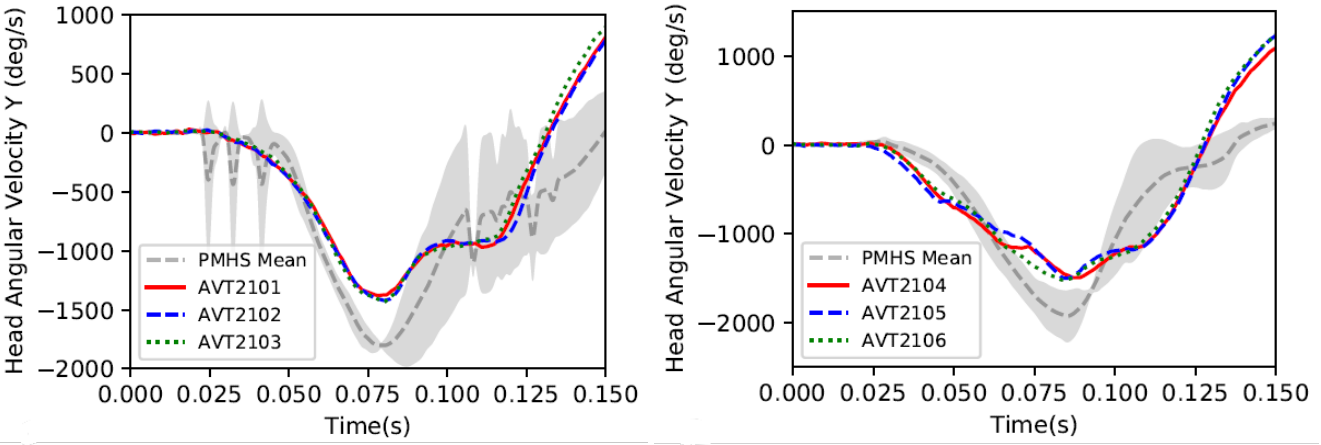

Fig. A11. Head angular velocity Y for the 25° (left) and 45° (right) configurations.

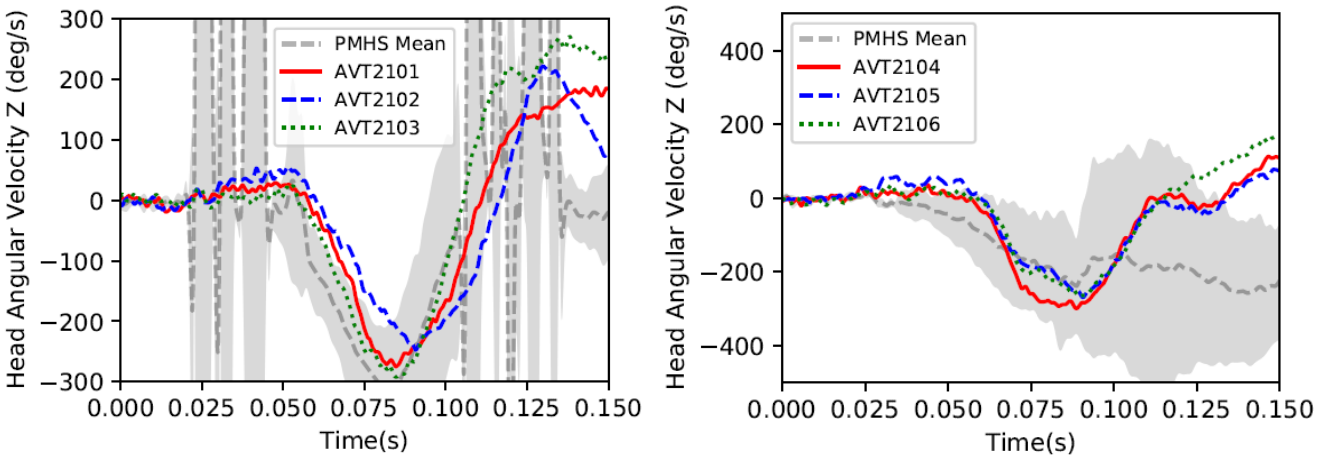

Fig. A12. Head angular velocity Y for the 25° (left) and 45° (right) configurations.

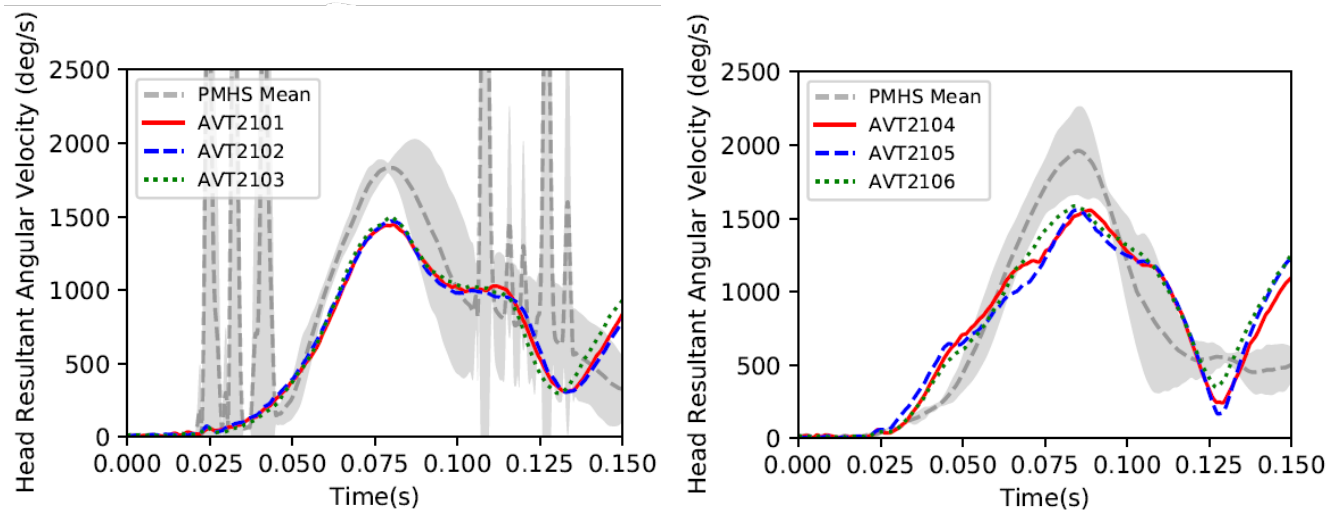

Fig. A13. Head resultant angular velocity for the 25° (left) and 45° (right) configurations.

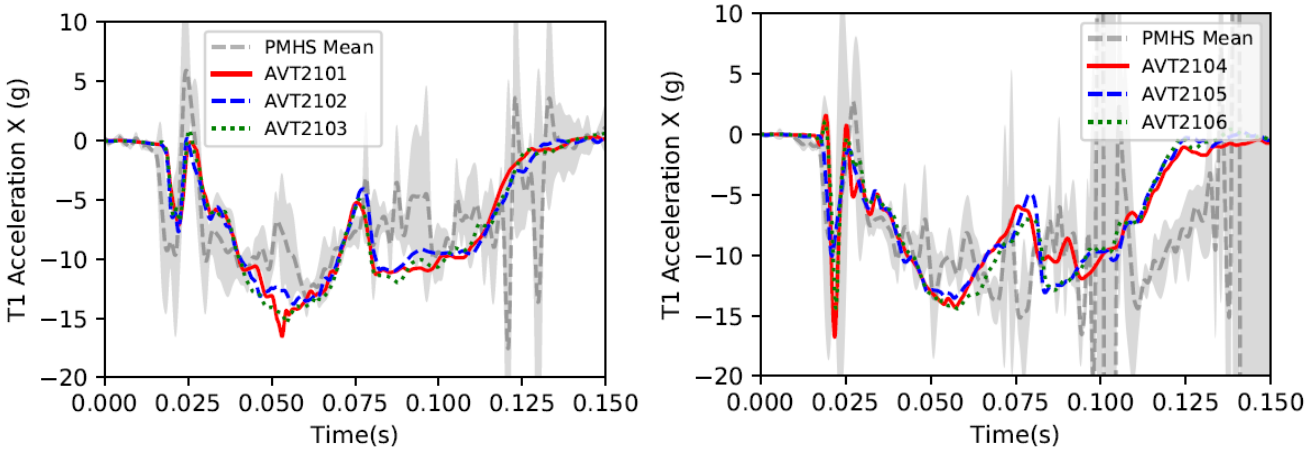

Fig. A14. T1 acceleration X for the 25° (left) and 45° (right) configurations.

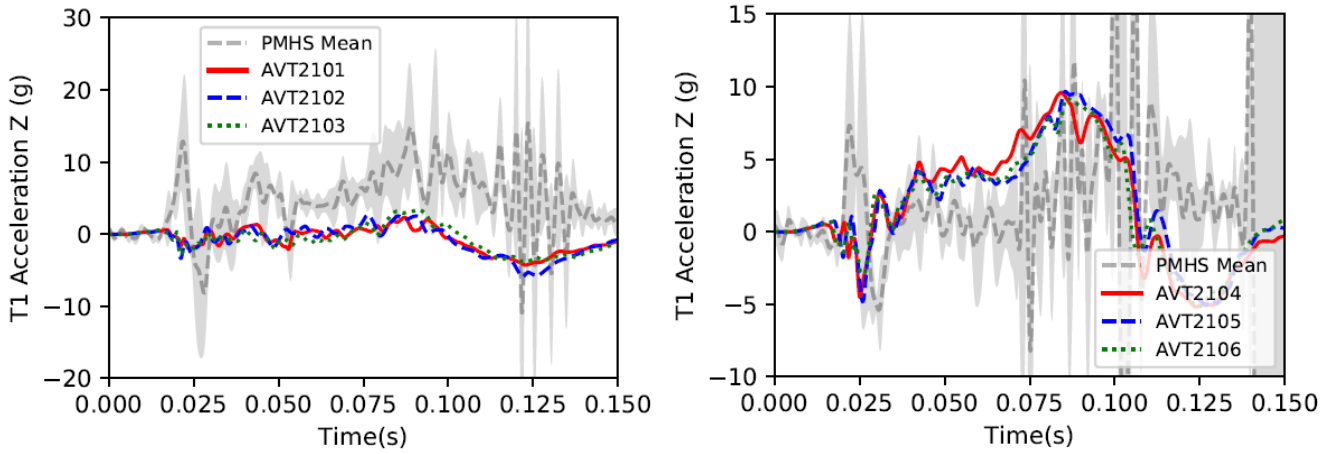

Fig. A15. T1 acceleration Z for the 25° (left) and 45° (right) configurations.

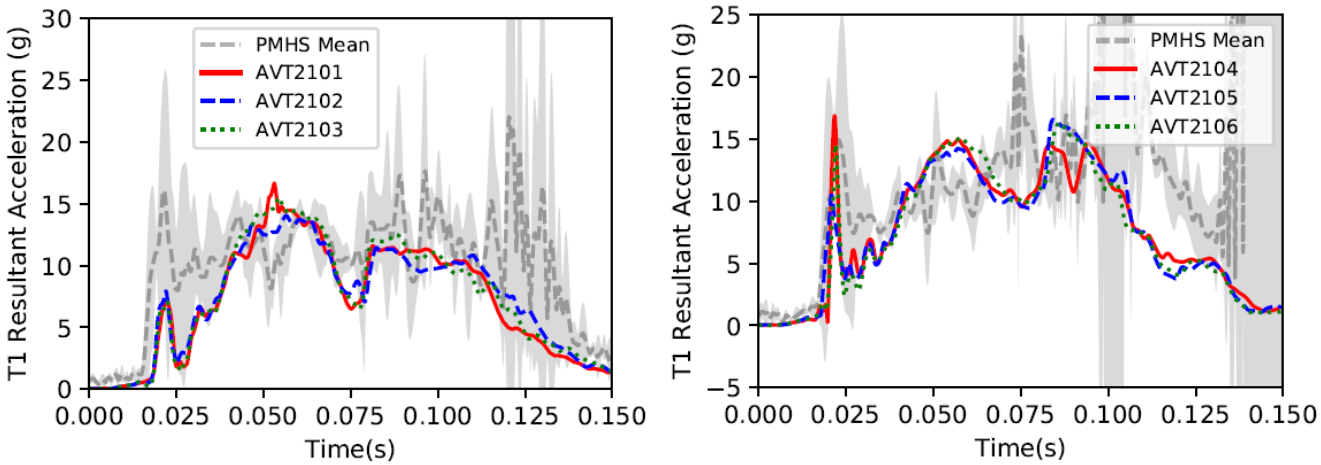

Fig. A16. T1 resultant acceleration for the 25° (left) and 45° (right) configurations.

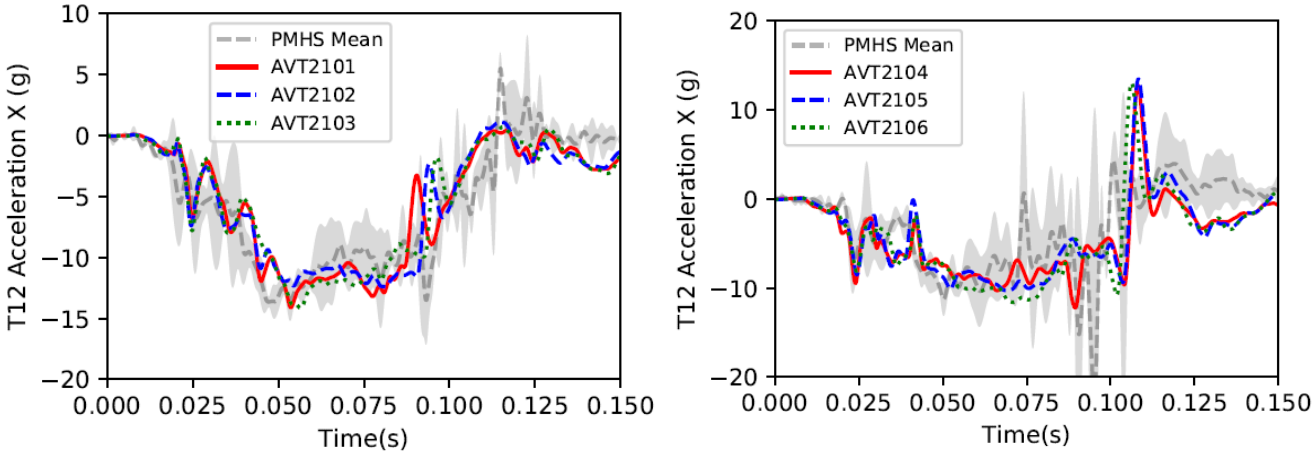

Fig. A17. T12 acceleration X for the 25° (left) and 45° (right) configurations.

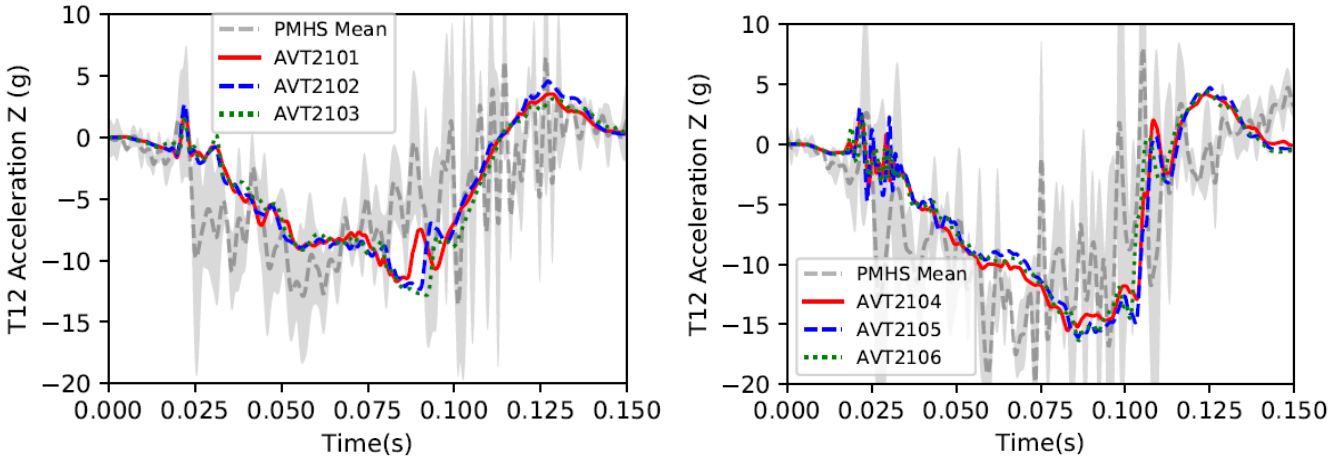

Fig. A18. T12 acceleration Z for the 25° (left) and 45° (right) configurations.

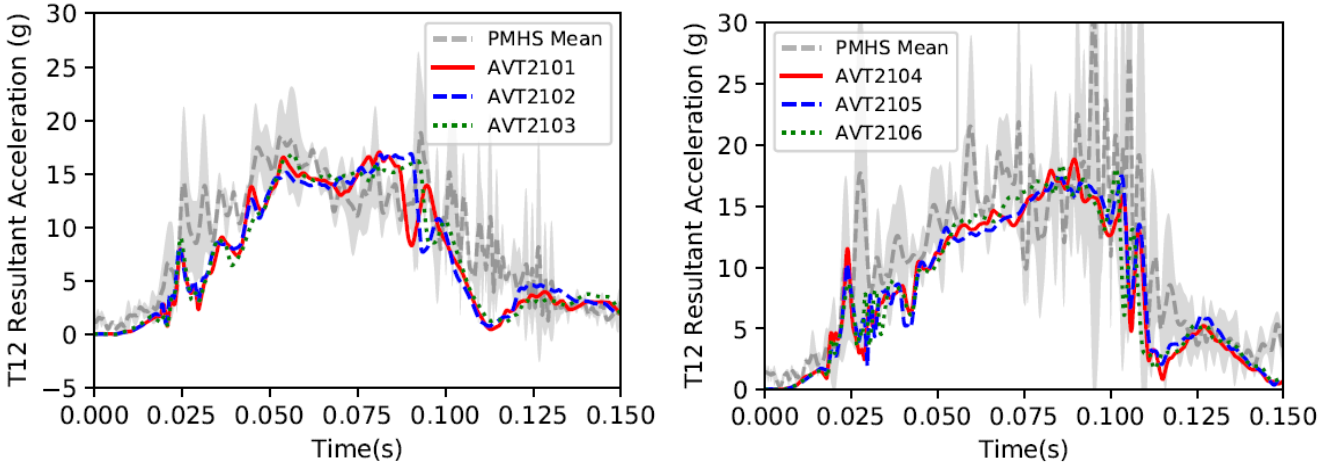

Fig. A19. T12 resultant acceleration for the 25° (left) and 45° (right) configurations.

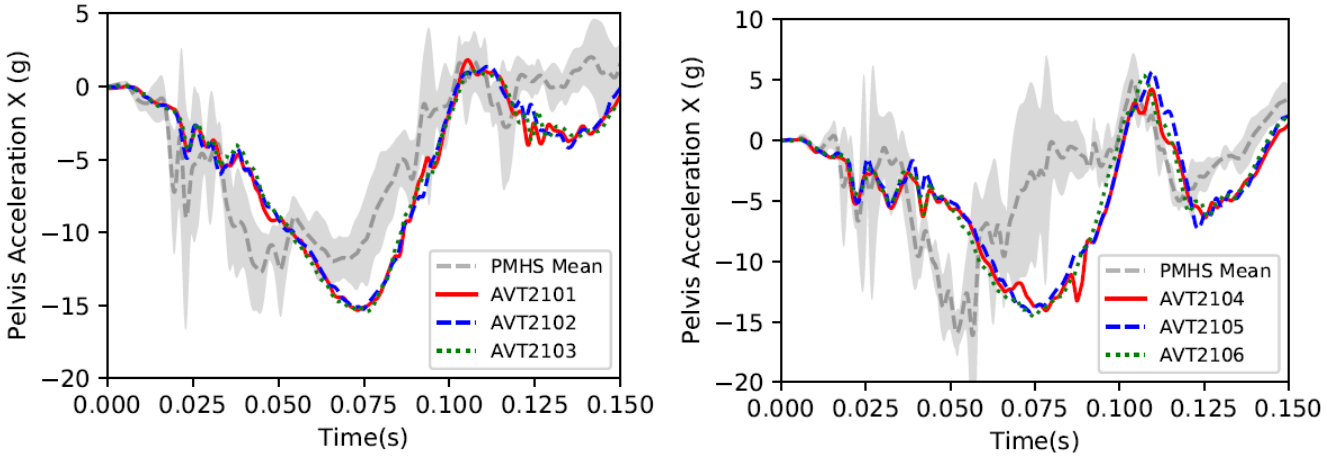

Fig. A20. Pelvis acceleration X for the 25° (left) and 45° (right) configurations.

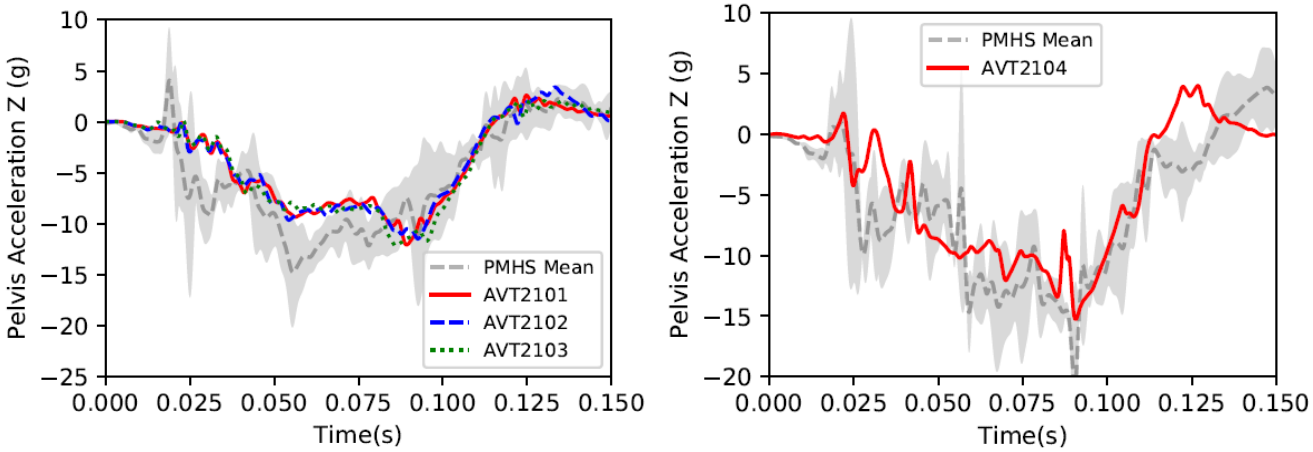

Fig. A21. Pelvis acceleration Z for the 25° (left) and 45° (right) configurations. Pelvis z-acceleration data were lost for test AVT2105 and AVT2106.

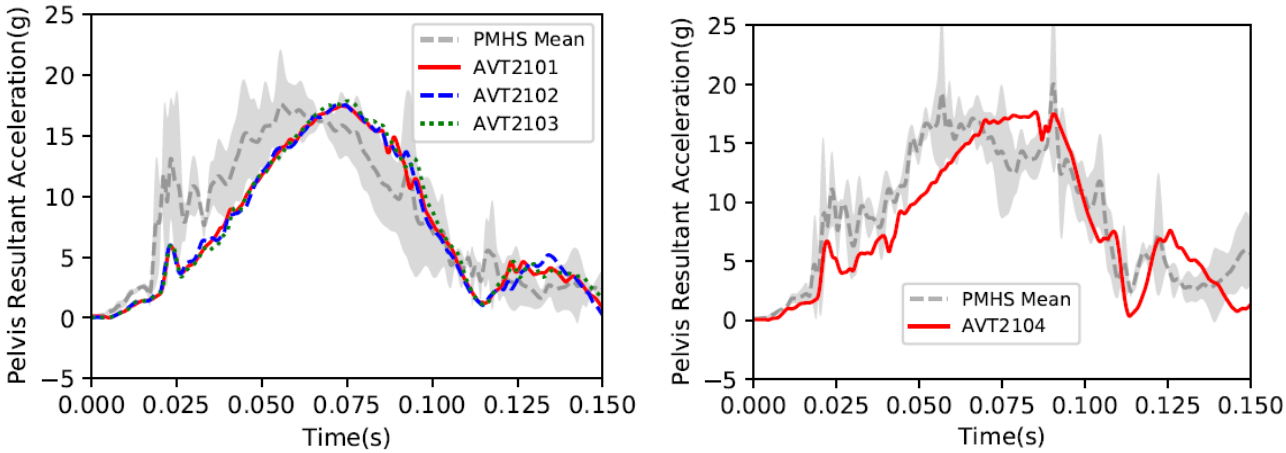

Fig. A22. Pelvis resultant acceleration for the 25° (left) and 45° (right) configurations.

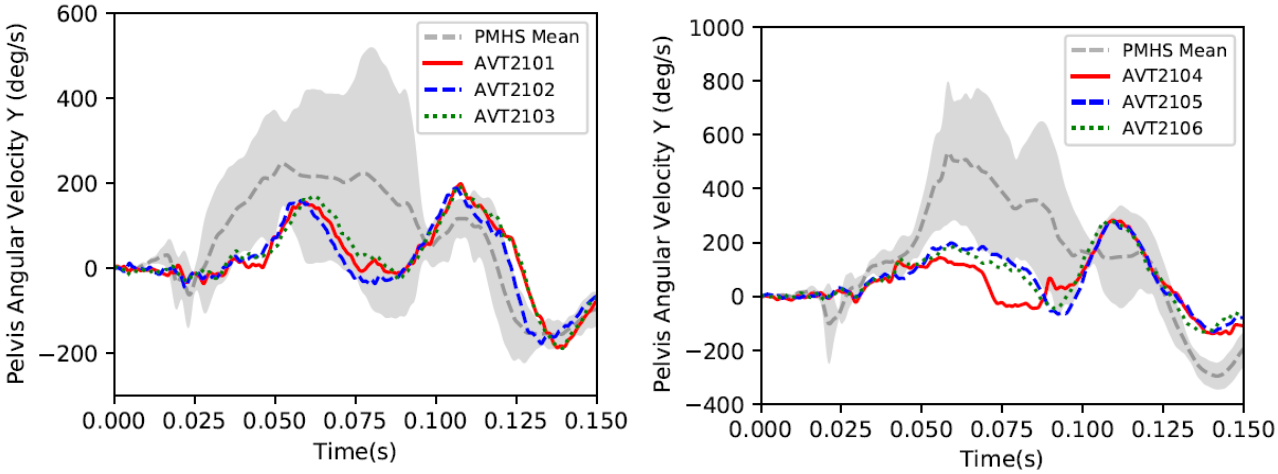

Fig. A23. Pelvis angular velocity Y for the 25° (left) and 45° (right) configurations.

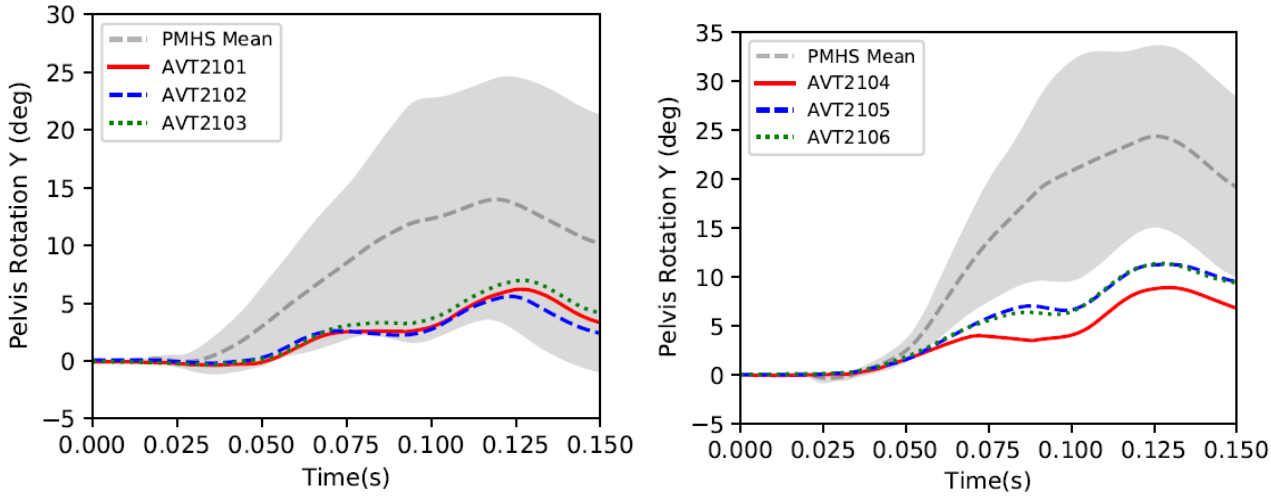

Fig. A24. Pelvis rotation Y for the 25° (left) and 45° (right) configurations.

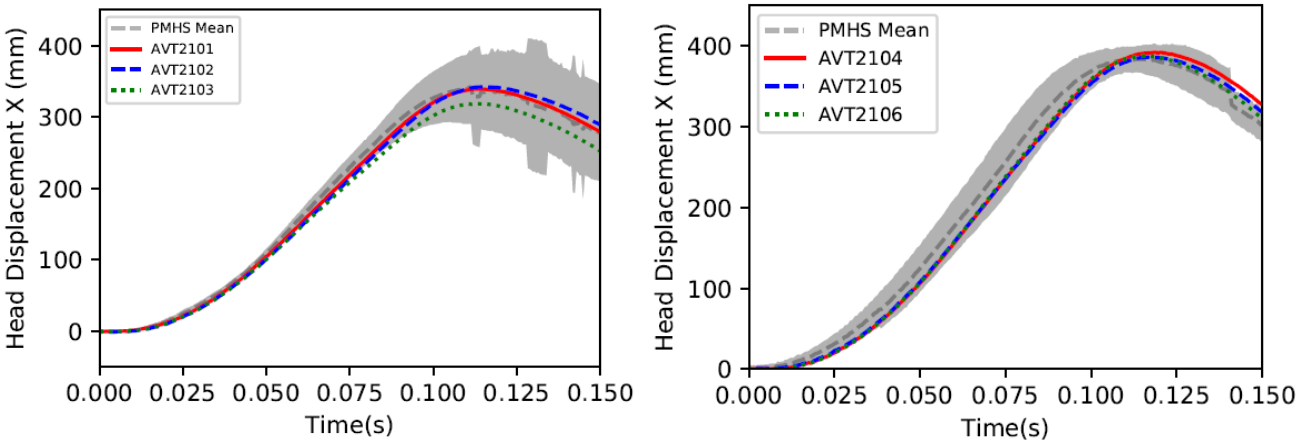

Fig. A25. Head displacement X for the 25° (left) and 45° (right) configurations.

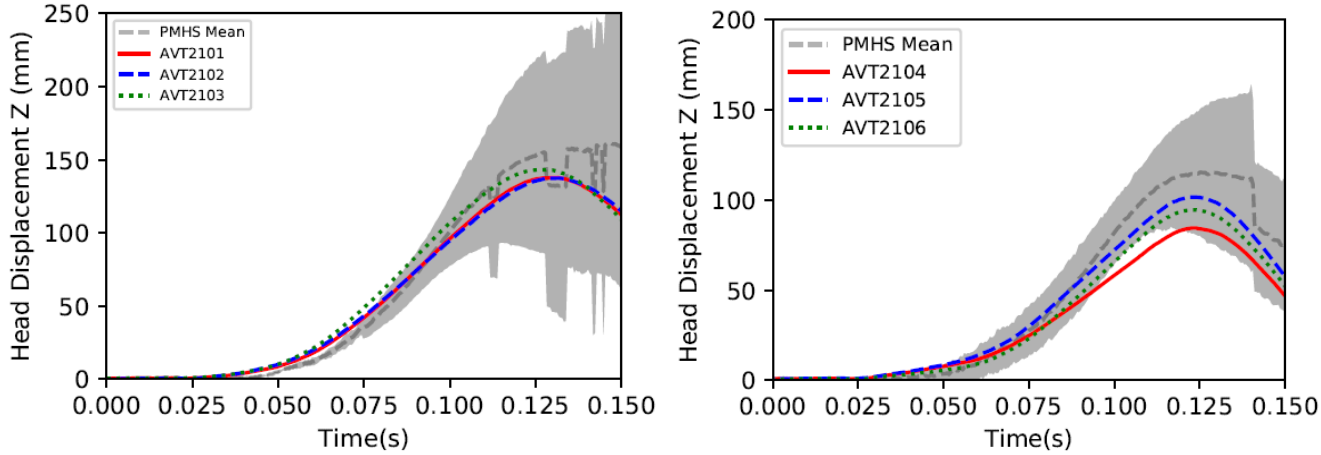

Fig. A26. Head displacement Z for the 25° (left) and 45° (right) configurations.

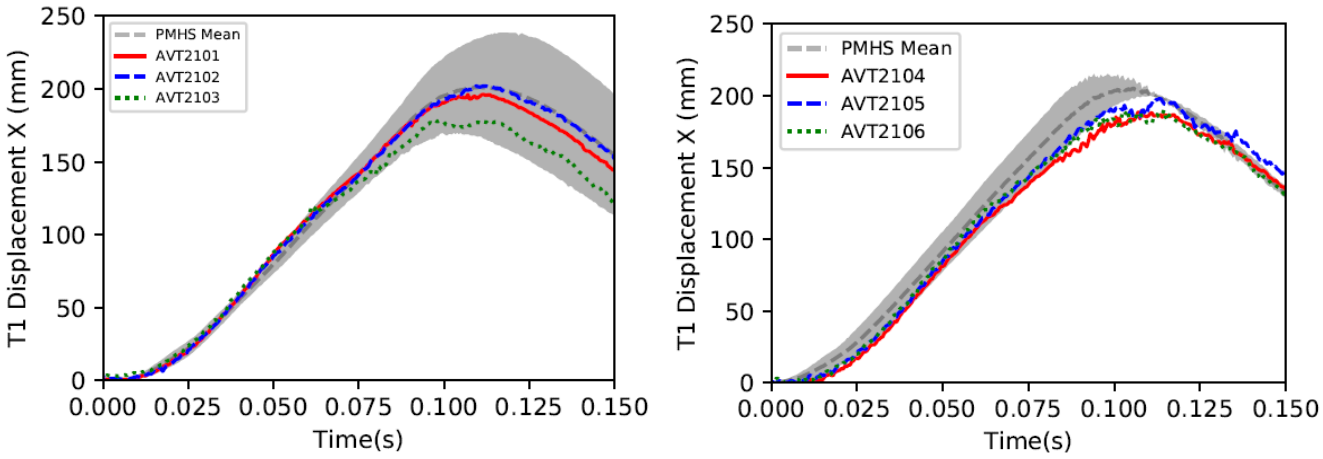

Fig. A27. T1 displacement X for the 25° (left) and 45° (right) configurations.

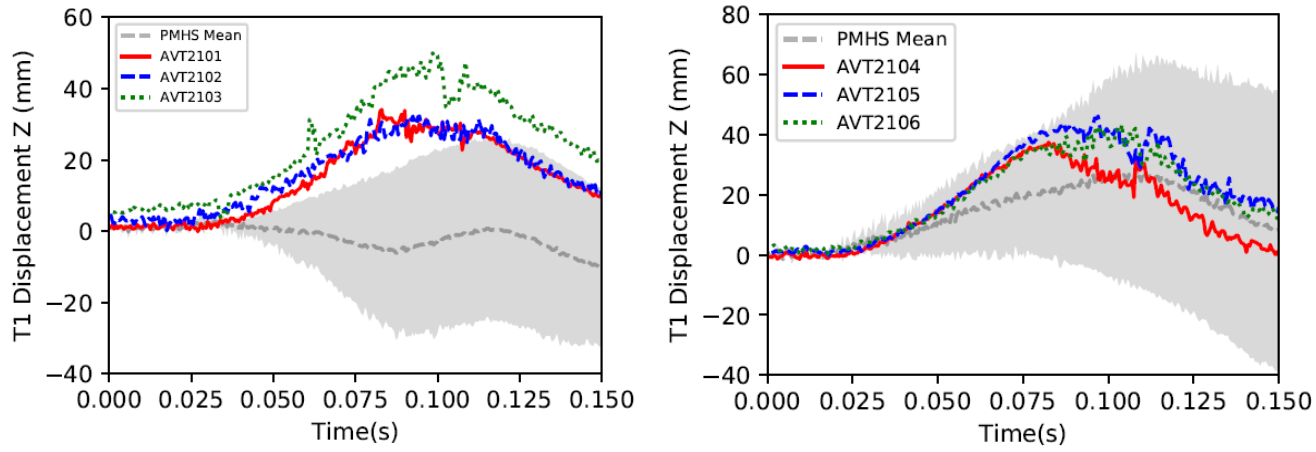

Fig. A28. T1 displacement Z for the 25° (left) and 45° (right) configurations.

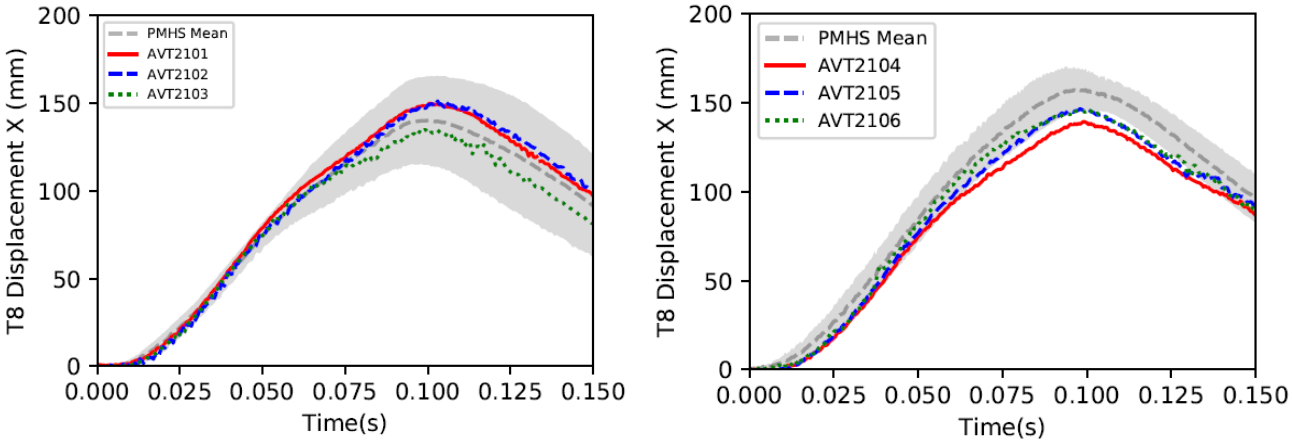

Fig. A29. T8 displacement X for the 25° (left) and 45° (right) configurations.

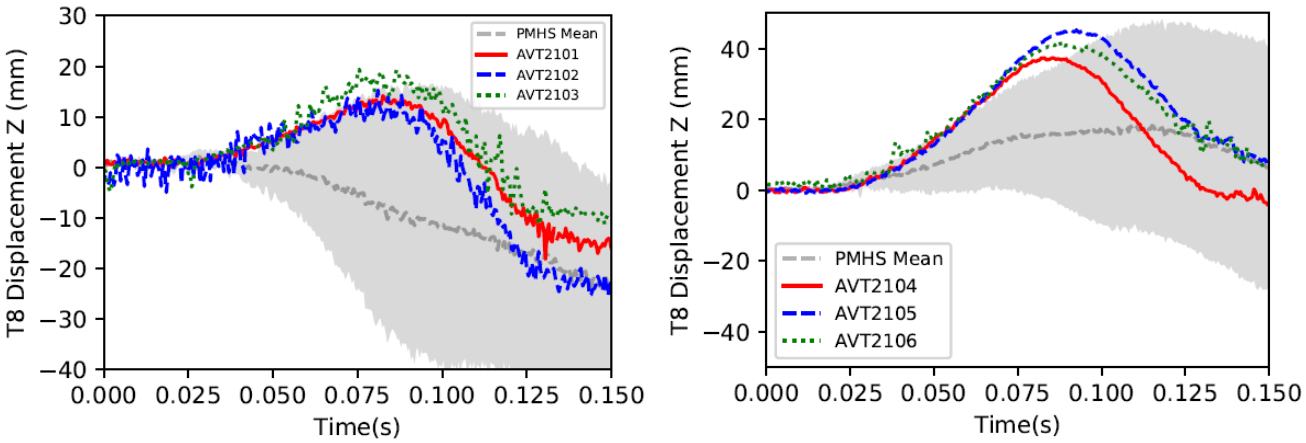

Fig. A30. T8 acceleration Z for the 25° (left) and 45° (right) configurations.

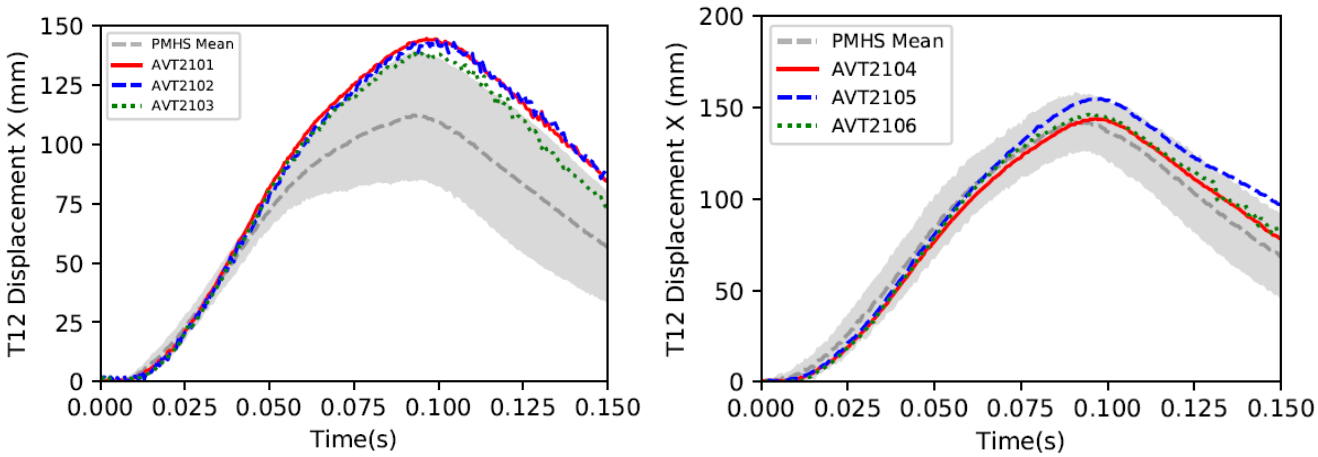

Fig. A31. T12 acceleration X for 25° (left) and 45° (right) configurations.

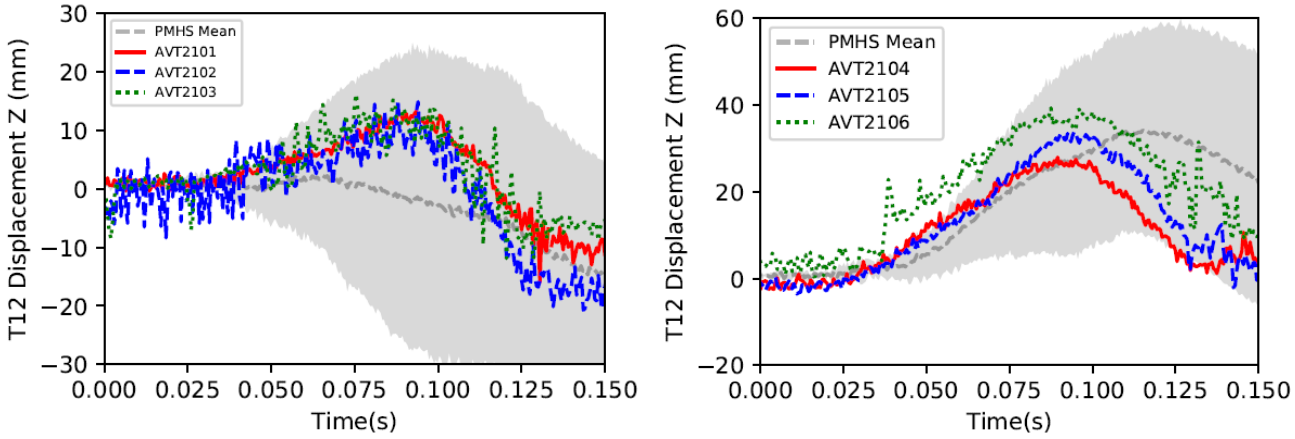

Fig. A32. T12 displacement Z for the 25° (left) and 45° (right) configurations.

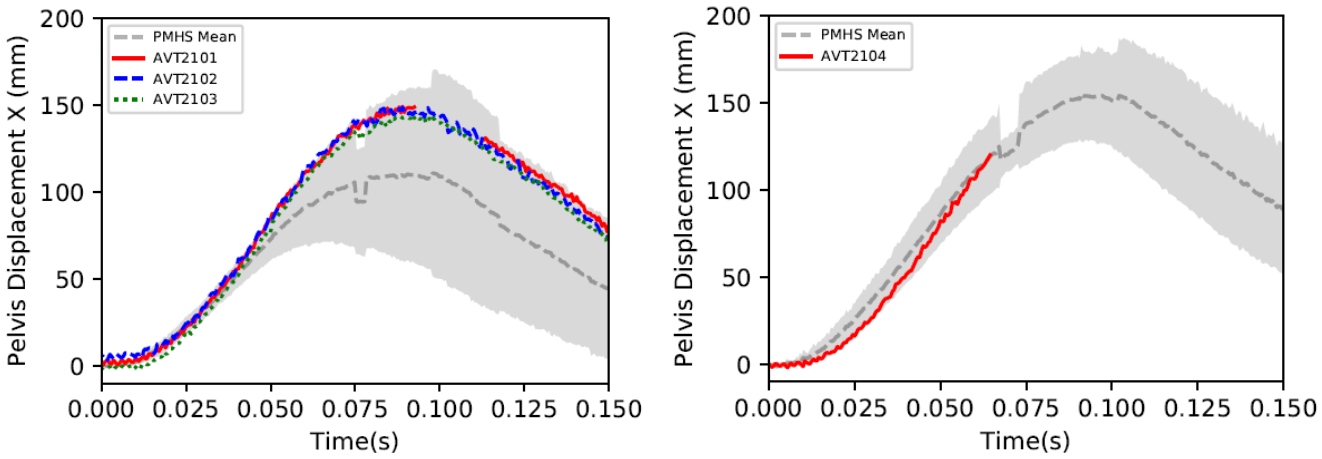

Fig. A33. Pelvis displacement X for the 25° (left) and 45° (right) configurations.

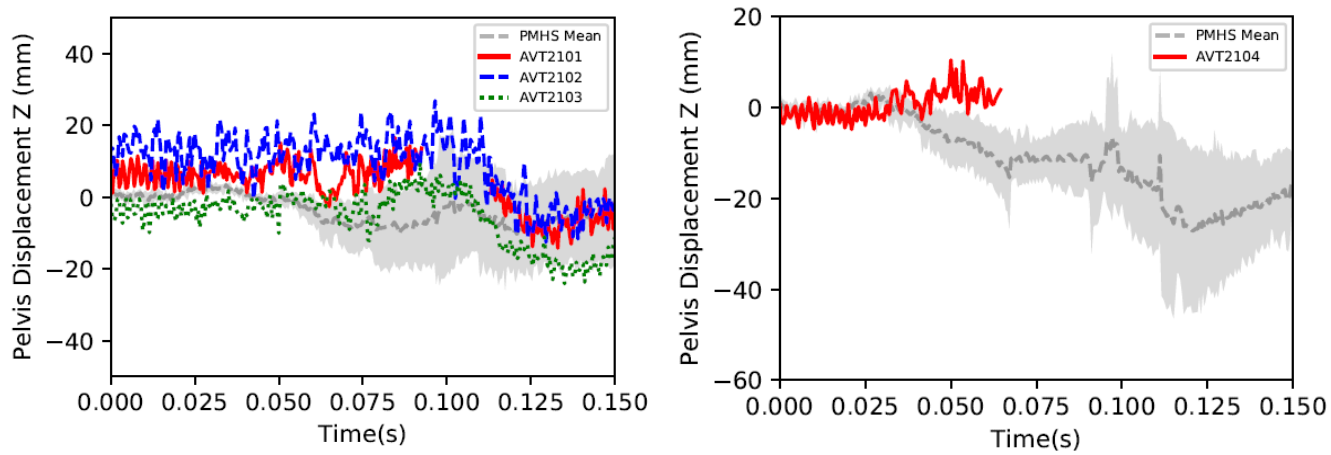

Fig. A34. Pelvis displacement Z for the 25° (left) and 45° (right) configurations.